Current Plant Biology xxx (2015) xxx–xxx

Contents lists available at ScienceDirect

Current Plant Biology

journal homepage: www.elsevier.com/locate/cpb

Time-dependent, glucose-regulated *Arabidopsis* Regulator of G-protein Signaling 1 network

Dinesh Kumar Jaiswal[a], Emily G. Werth[b], Evan W. McConnell[b], Leslie M. Hicks[b,**], Alan M. Jones[a,c,*]

[a] Department of Biology, University of North Carolina, Chapel Hill, NC 27599, USA
[b] Department of Chemistry, University of North Carolina, Chapel Hill, NC 27599, USA
[c] Department of Pharmacology, University of North Carolina, Chapel Hill, NC 27599, USA

ARTICLE INFO

Article history:
Received 29 October 2015
Accepted 17 November 2015

Keywords:
Heterotrimeric G-protein
Membrane protein complexes
Tandem affinity purification
Mass spectrometry
Glucose signaling

ABSTRACT

Plants lack 7-transmembrane, G-protein coupled receptors (GPCRs) because the G alpha subunit of the heterotrimeric G protein complex is "self-activating"—meaning that it spontaneously exchanges bound GDP for GTP without the need of a GPCR. In lieu of GPCRs, most plants have a seven transmembrane receptor-like regulator of G-protein signaling (RGS) protein, a component of the complex that keeps G-protein signaling in its non-activated state. The addition of glucose physically uncouples AtRGS1 from the complex through specific endocytosis leaving the activated G protein at the plasma membrane. The complement of proteins in the AtRGS1/G-protein complex over time from glucose-induced endocytosis was profiled by immunoprecipitation coupled to mass spectrometry (IP-MS). A total of 119 proteins in the AtRGS1 complex were identified. Several known interactors of the complex were identified, thus validating the approach, but the vast majority (93/119) were not known previously. AtRGS1 protein interactions were dynamically modulated by D-glucose. At low glucose levels, the AtRGS1 complex is comprised of proteins involved in transport, stress and metabolism. After glucose application, the AtRGS1 complex rapidly sheds many of these proteins and recruits other proteins involved in vesicular trafficking and signal transduction. The profile of the AtRGS1 components answers several questions about the type of coat protein and vesicular trafficking GTPases used in AtRGS1 endocytosis and the function of endocytic AtRGS1.

© 2015 The Authors. Published by Elsevier B.V. This is an open access article under the CC BY-NC-ND license (http://creativecommons.org/licenses/by-nc-nd/4.0/).

1. Introduction

The *Arabidopsis* G-proteins, despite having a simpler repertoire than that in metazoans, impart many physiological and biochemical responses and affect growth and development in plants [1]. In metazoans, the duration of G-protein signal termination is dependent on (1) the residence time of the GPCR agonist, (2) the number of activating interactions between the cognate GPCR coupled to the G protein complex over time and (3) the rate of deactivation through intrinsic GTPase activity of the Gα protein. The latter is accelerated by interaction with a group of regulator of G protein signaling (RGS) proteins, accelerating hydrolysis of $G_{\alpha GTP}$ into $G_{\alpha GDP}$ and returning the G protein complex to the resting state [2]. It is now well established that plants use a distinct mechanism to regulate G-protein signaling from metazoans and differ in many aspects. First, plant cells lack G-protein coupled receptors (GPCR) that stimulate guanine nucleotide exchange. Second, plant Gα proteins exchange guanine nucleotides spontaneously *in vitro*. Third, all plants, except the cereals, contain a receptor-like RGS protein that deactivates until decoupled from the G protein complex. In *Arabidopsis*, the RGS protein (AtRGS1) has a seven transmembrane (7TM) domain at its N-terminus and a catalytic RGS box at its C-terminal domain [3–7].

The mechanism of glucose-induced G protein activation is known. Urano et al. demonstrated that D-glucose recruits WITH NO LYSINE (WNK) kinases to phosphorylate AtRGS1 and that this phosphorylation is necessary and sufficient for endocytosis [7,8]. AtRGS1 endocytosis leads to physical uncoupling of AtRGS1 from the *Arabidopsis* G protein α subunit (AtGPA1) and thus a release of the GAP activity and concomitant sustained activation of G-protein signaling. One of the most intriguing aspects of

* Corresponding author at: Department of Biology, CB# 3280 Coker Hall, University of North Carolina, Chapel Hill, USA. Fax: +1 919 962 1625.
** Corresponding author at: Department of Chemistry, CB# 3290 Kenan A221, University of North Carolina, Chapel Hill, USA. Fax: +1 919 962 2388.
E-mail addresses: lmhicks@unc.edu (L.M. Hicks), alan_jones@unc.edu (A.M. Jones).

http://dx.doi.org/10.1016/j.cpb.2015.11.002
2214-6628/© 2015 The Authors. Published by Elsevier B.V. This is an open access article under the CC BY-NC-ND license (http://creativecommons.org/licenses/by-nc-nd/4.0/).

glucose-regulated, AtRGS1-mediated G-protein activation is that the response is receptive to both signal concentration and timing information, unlike G-protein signaling in animals which is triggered by a threshold of signal [8]. This emergent property has dose and duration reciprocity such that an acute dose of glucose (*e.g.* 6%) induces complete AtRGS1 endocytosis in 30 min while a low dose induces endocytosis over many hours [8]. While AtRGS1 is considered an inhibitor of G-protein signaling as a GTPase Activating Protein (GAP), the effect of genetic ablation of AtRGS1 suggests that AtRGS1 is a positive regulator of G-protein signaling [9]. Given that trafficking of AtRGS1 is an important part of plant G protein signaling, we hypothesized that signaling through AtRGS1 is both time and sub-cellular location contingent. Specifically, AtRGS1 signaling from the endosome may be an obligatory aspect of signaling output as has been recently shown for β2-adrenoceptor-mediated signaling [10].

Studies of plant G-proteins in the last decade revealed associations with fundamental biological processes such as sugar perception [11,7], organ development [12], hormone signaling [13,14], light responsiveness [15], biotic and abiotic stress [16–19,6], among others. Sugar-induced signal transduction pathways play significant roles in many physiological processes in plants such as photosynthetic efficiency [20], cell wall hexose composition [21], and pathogen defense [22,23]. AtRGS1 plays an important role not only in sugar-mediated seedling development [5], but also in responses to environmental cues [18].

While the heterotrimeric plant G-protein complex is similar in atomic structure to that from animal cells [24], the mechanism of activation of G-protein signaling is dramatically different [1]. Activation involves unknown proteins that operate on the core complex. Targets of the activated G protein complex as defined for animal cells are mostly lacking in plant cells. Therefore, a yeast complementation was previously conducted to assemble a set of candidate targets of G protein complex proteins, but that analysis clearly indicated that the screen was not saturated [25]. Moreover, yeast complementation only detects direct interactions between bait and prey although indirect interactions can be deduced from an *in silico* construction of the network. Finally, while post-translational modifications are often critical for protein–protein interactions, complementation screens in yeast are insensitive to modifications such as the phosphorylation state [26].

For these reasons, it was necessary to initiate an *ab initio* approach to discover the missing elements to G protein signaling in plant cells. Here we used tandem affinity purification that leads to highly enriched samples for AtRGS1-containing complexes. Since AtRGS1 regulates the activation state of G-proteins in a time-dependent manner, we sought *in planta* interacting proteins of AtRGS1 over time after induction with glucose. Mass spectrometry analyses of purified protein complexes led to the identification of 119 interacting AtRGS1 complex proteins associated with diverse biological functions such as response to stimulus, cell organization, transport, and metabolism.

2. Materials and methods

2.1. Plant materials, seedling growth and sugar treatment

All the wild type plants and mutant alleles used in this study were in the Col-0 ecotype of *Arabidopsis thaliana*. The ORF of AtRGS1 and AtRGS1(E320K) were cloned into pEarleyGate 205 vector. The 35S:RGS1-TAP and 35S:RGS1(E320K)-TAP overexpressing lines in the *rgs1-2* background were generated by the floral dip method [27]. ACD2-TAP transgenic lines were described by Sakuraba et al. [28]. Seeds of *Arabidopsis* were surface sterilized and sugar treatments given as described earlier [7,9]. Sterilized and stratified *Arabidopsis* seeds were grown for seven days in flasks containing quarter-strength MS liquid media, subjected to two days sugar starvation in the dark and then treated with 6% glucose for 0, 10 and 30 min. Two hours before sugar treatment, seedlings were treated with 70 μM cycloheximide to block protein translation. The flasks were grown hydroponically in a constant low light (50 $\mu mol\, s^{-1}\, m^{-2}$) growth chamber at 23 °C with gentle rotation (120 rpm).

2.2. Confocal microscopy and AtRGS1 internalization

All confocal microscopy analyses were performed using a Zeiss LSM710 confocal laser scanning microscope equipped with a C-Apochromat × 40 NA = 1.20 water immersion objective. The imaging and fluorescence internalization were analyzed using ImageJ software as previously described [7].

2.3. Isolation of total membranes and tandem affinity purification

Approximately 10 gm of seedlings (non-treated and 6% glucose-treated for 10 min and 30 min) were ground into powder in liquid nitrogen. The tissue powder was homogenized in a Waring Blender homogenizer with small size 30-mL bowl (Waring, USA) around 18000 rpm speed for 10–15 s with homogenizing buffer [50 mM Tris–Cl (pH 8.0), 150 mM NaCl, 10 mM EDTA (ethylenediaminetetraacetic acid), 1 mM PMSF (phenylmethylsulfonyl fluoride), 2 mM DTT (dithiothreitol), 0.1% Protease inhibitor cocktail Sigma]. The cell debris was filtered through one-layer of Miracloth (Calbiochem) and the filtrate was centrifuged at 12,000 × *g* for 15 min at 4 °C. The supernatant was recovered and centrifuged at 100,000 × *g* for 1 h at 4 °C. The resulting pellet containing the membrane fraction was suspended in detergent containing membrane suspension buffer [50 mM Tris–Cl (pH 8.0), 150 mM NaCl, 10 mM EDTA, 1 mM PMSF, 2 mM DTT, 0.5–1% detergent (as indicated), 0.1% Protease inhibitor cocktail Sigma]. The suspension was rotated overnight at 4 °C [29], and then centrifuged for 15 min to separate the insoluble debris from solubilized protein. The protein concentration of the solubilized fraction was estimated using an ESL (Exact, Sensitive, Low Interference) protein assay kit (Roche Molecular Biochemicals) and diluted to 1 mg/ml. The IgG-agarose beads were washed three times with membrane suspension buffer and then mixed with the diluted protein fraction (100 μl slurry for 1 mL solubilized protein) and incubated for 4 h at 4 °C on gentle rotation. After incubation, samples were briefly spun at 2000 × *g* for 1 min and supernatants were collected. The IgG-agarose beads were washed three times with membrane suspension buffer and then incubated with Tobacco Etch Virus (TEV) protease in the same buffer (0.5% detergent) for 2 h at room temperature (22 °C). His6-tagged TEV protease was purified as described previously [30]. After incubation, samples were briefly spun at 2000 × *g* for 1 min and the supernatants were recovered. Before proceeding to the next step of purification, the EDTA present in eluates was equilibrated by adding $CaCl_2$. Calmodulin-sepharose beads were washed three times with calmodulin-binding buffer [50 mM Tris–Cl (pH 8.0), 150 mM NaCl, 1 mM Mg-acetate, 2 mM $CaCl_2$, 2 mM DTT, 0.5% ASB-14] and then eluate was mixed and incubated for 2 h at 4 °C on gentle rotation. After incubation, samples were briefly spun at 2000 × *g* for 1 min and the supernatants were collected and calmodulin-sepharose beads were washed three times with calmodulin-binding buffer. Bound complexes were eluted with 200 μl of calmodulin elution buffer [50 mM Tris–Cl (pH 8.0), 150 mM NaCl, 1 mM magnesium acetate, 2 mM $CaCl_2$, 2 mM DTT, 2 mM EGTA (ethylene glycol tetra acetic acid), 1% ASB-14].

Please cite this article in press as: D.K. Jaiswal, et al., Time-dependent, glucose-regulated *Arabidopsis* Regulator of G-protein Signaling 1 network, Curr. Plant Biol. (2015), http://dx.doi.org/10.1016/j.cpb.2015.11.002

2.4. SDS-PAGE and Western blotting

The purified protein complexes were pooled and precipitated by chloroform/methanol as previously described [31]. The pellet was redissolved in buffer (7 M urea, 2 M thiourea and 1% ASB-14), diluted 1:1 in Laemmli buffer containing 4% β-mercaptoethanol and separated by 12% SDS PAGE. The proteins were detected by silver staining with the Pierce™ Silver Stain Kit per the manufacturer's instructions. For mass spectrometry analyses, protein complexes were separated on 12% SDS PAGE precast gels (Bio-Rad), stained with Sypro Ruby, and imaged using a Typhoon scanner (GE Healthcare). The apparent molecular weight was estimated using Precision Plus protein standards (Bio-Rad). Protein concentrations were determined with the Protein Assay ESL (Roche). For immunoblot analysis, proteins were blotted onto PVDF membranes (Bio-Rad) and blocked in 3–5% (v/v) milk powder in TBS buffer for at least 1 h at room temperature and then incubated overnight at 4 °C with different primary antibodies. Protein bands were detected with horseradish peroxidase-conjugated IgG diluted 1/10,000 (Amersham Biosciences) as per the manufacturer's instruction (SuperSignal Western Blotting Kits, Thermo Scientific).

2.5. In-gel tryptic digestion, mass spectrometry, and protein identification

SYPRO Ruby stained protein bands were excised manually for downstream processing. The entire gel lane was processed accordingly. Gel slices were destained using 50 mM ammonium bicarbonate/50% acetonitrile (ACN) solution, reduced with 10 mM dithiothreitol (30 min, RT), alkylated with 55 mM iodoacetamide (30 min, RT, dark) and an in-gel trypsin digestion (25 ng trypsin in 50 mM NH_4HCO_3) was performed overnight at 37 °C as previously described [32]. Following digestion, peptides were extracted first with 1% formic acid in 2% ACN, and second with 60% ACN. Peptide extracts were dried by vacuum centrifugation and resuspended in 10 μl of 5% ACN/0.1% trifluoroacetic acid prior to separation using a nanoACQUITY UPLC (Waters, Milford, MA, USA) coupled to a TripleTOF 5600 MS/MS (AB Sciex, Framingham, MA, USA). Samples (5 μL) were injected onto a trap column (nanoACQUITY UPLC 2G-W/M Trap 5 μm Symmetry C18, 180 μm × 20 mm) at a flow rate of 5 μL/min for 5 min. Peptides were separated using a C18 column (nanoACQUITY UPLC 1.8 μm BEH, 75 μm × 250 mm) at a flow rate of 300 nL/min. Mobile phase A consisted of 0.1% formic acid in H_2O and mobile phase B was 0.1% formic acid in ACN. Peptides were separated using a 30-min linear gradient from 5% to 30% mobile phase B. MS data acquisition was performed as previously described [33]. Raw mass spectral files were converted to mascot generic format (*.mgf) using the ProteinPilot algorithm (AB Sciex). All LC-MS/MS files for bands from the same gel lane were merged into a single peak list and protein identification was performed using a Mascot Server (Matrix Science, London, UK; v2.5.1) against the *A. thaliana* UniProtKB database (Proteome ID: UP000006548, 31,527 entries; accessed July 15, 2015) appended with sequences for common laboratory contaminants (http://www.thegpm.org/cRAP/, 116 entries). Searches of MS/MS data used trypsin protease specificity with the possibility of up to 2 missed cleavages, peptide mass tolerance of 20 ppm, and MS/MS ion mass tolerance of 0.8 Da. Acetylation of the protein N-terminus, carbamidomethylation of cysteine, deamidation of asparagine/glutamine, and oxidation of methionine were selected as variable modifications. Significant peptide identifications above the identity or homology threshold were adjusted in Mascot to ≤1% peptide FDR and resulting matches were exported for data processing. The raw mass spectrometry data were deposited into the ProteomeXchange Consortium *via* the PRIDE partner repository with the dataset identifier PXD003103 and 10.6019/PXD003103.

2.6. SAINT and bioinformatic analysis

ProHits Lite VM v3.0.3 [34] was used to parse result files for proteins with ≥2 unique peptides and format input files for protein–protein interaction analysis. A significance analysis of interactome algorithm (SAINTexpress v3.6.1) [35] was run under default settings to identify proteins that were statistically enriched. Data sets from the AtRGS1 purifications were analyzed using appropriate negative controls, *i.e.*, ACD2-TAP and Col-0 plants without expression of TAP tag. Negative control replicates were treated as different baits to improve statistical performance of the SAINT algorithm [36]. Known contaminants (http://www.thegpm.org/crap/index.html) were removed before SAINT analysis (see Section 3.4). We only considered prey proteins detected with probability avgP ≥ 0.3 for further inspection. Network visualization was performed using Cytoscape v3.2.1 [37] where edge thickness is proportional to the average probability (avgP) for each bait-prey interaction detected.

To define the functional annotation of the identified candidate proteins obtained after SAINT analysis, gene ontology (GO) analysis was performed using PlantGSEA (Plant GeneSet Enrichment Analysis) [38]. The GO terms and gene families enrichments were detected using Fisher's test with Yekutieli correction (false discovery rate cutoff of 0.05). *Arabidopsis* whole genome annotation was used as the background. The data were visualized using REVIGO [39].

2.7. Mating-based split ubiquitin system

Mating-based split ubiquitin assays were performed as previously described [40]. Entry clones of selected candidate proteins, namely, ras-related protein RABB1c (At4g17170), 14-3-3-like protein GF14 phi (At1g35160), aquaporin PIP2-1 (At3g53420), guanylate-binding protein (GBP, At1g03830), ADP-ribosylation factor A1E (At3G62290), mitochondrial outer membrane protein porin 1 (VDAC1, At3g01280), and 3 (VDAC3, At5g15090) were obtained from ABRC. They were subsequently mobilized by LR recombination [Gateway LR Clonase Enzyme Mix (Invitrogen, USA)] into Nub destination vectors (pNX32_GW). The AtRGS1 ORF was subsequently mobilized by LR recombination into pMetYC-GW, to generate the C-terminal Cub fusions of AtRGS1. Empty vectors were used as negative controls. The Cub and Nub clones were transformed into *Saccharomyces cerevisiae* haploid strains THY.AP4 and THY.AP5, respectively [41]. Clones from each THY.AP5 and THY.AP4 transformation were mixed and used for subsequent interaction assays. The protein interactions were detected by assessment of growth of the diploid cells on selective medium lacking leucine, tryptophan, histidine and adenine supplemented with various concentrate of methionine (200 μM and 1 mM).

3. Results

3.1. Detergent screening and tandem affinity purification of AtRGS1-associated proteins

We first investigated whether the AtRGS1–TAP protein was functional. To test this genetically, we ectopically expressed AtRGS1–TAP lines in the *rgs1*-2 null mutant and found that *rgs1*-2 phenotypes were rescued to wild type (Fig. 1). This indicates that the AtRGS1–TAP protein was folded properly and functional *in vivo*. Our approach involved isolation of proteins from a lipid environment, therefore it was necessary to optimize detergent solubilization. AtRGS1 has an N-terminal seven-transmembrane

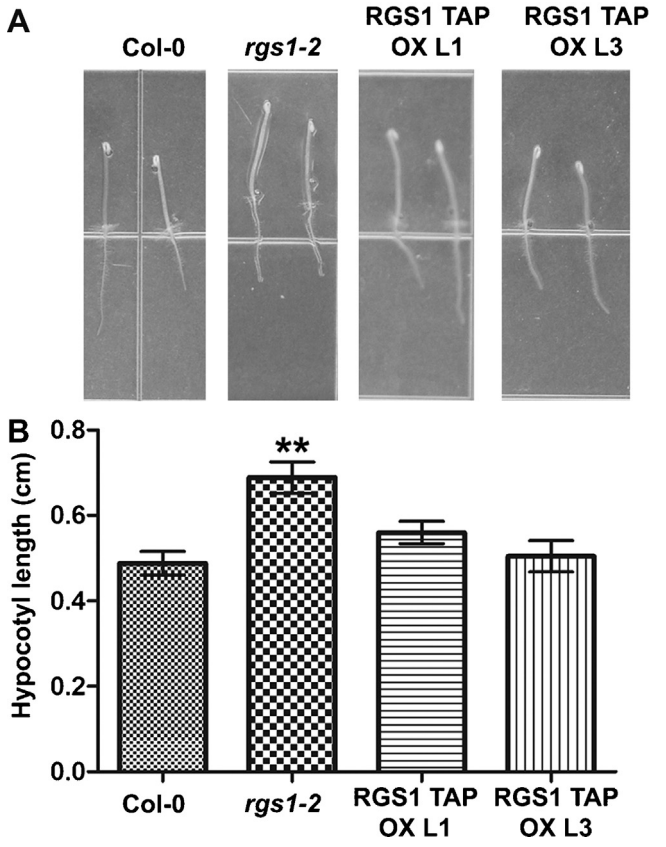

Fig. 1. Genetic complementation of the *rgs1-2* null mutant with AtRGS1-TAP. (A) Representative images of hypocotyl growth (mm) of plants for each genotype on ¼ X-strength MS with 1% (w/v) sucrose at 3 days. (B) Quantitation of hypocotyl growth measured at 3 days. ANOVA was used to determine statistical difference ($p < 0.05$, $n \geq 10$). RGS1-TAP OX L1 and RGS1-TAP OX L3 represents *rgs1-2* complemented line 1 and line 3 by ectopically expressing 35S:AtRGS1–TAP construct.

(7TM) helical domain and it is known that membrane protein complexes are sensitive to the detergents used during purification. Therefore, we first needed to determine which detergents should be used for the purification of the AtRGS1 protein complex and then optimize effective tandem affinity purification procedures. We systematically evaluated 5 detergents [*n*-dodecyl-β-D-maltopyranoside (DDM), amidosulfobetaine-14 (ASB-14), Nonidet P-40 (NP-40), *n*-Octyl-*b*-D-glucopyranoside (OG) and Triton X-100] to define the minimum concentration needed to maximally solubilize AtRSG1 (Fig. 2A). ASB-14 is a sulfobetaine-type zwitterionic detergent, while DDM, NP-40, OG and Triton-X100 are all nonionic detergents. The critical micelle concentration (CMC) for ASB-14 is 8 mM, whereas DDM, NP-40, OG and Triton-X100 are 0.17, 0.29, 23 and 0.22 mM, respectively. It has been shown that DDM, NP40 and Triton X-100 are used to solubilize tagged membrane proteins in yeast [42], whereas OG and ASB-14 for solubilizing plant proteins [43,7]. For each of these treatments, we screened by Western blotting to detect the AtRGS1 protein (Fig. 2A). These detergents were used at 0.5% and 1% concentration. The tested detergents displayed different efficiency in the solubilization of AtRGS1 and we concluded that ASB-14 and DDM were the most effective detergents in solubilizing the tagged bait protein (Fig. 2A). To determine if ASB14 at 1% is overly stringent, we determined if known components of the complex were stripped by the detergent. As shown in Fig. 2B, the ASB-14 solubilized complex contains AtRGS1, the Gα subunit (AtGPA1), and the Gβ subunit (AGB1). Therefore, ASB-14 (1%) was chosen for purification in the subsequent large-scale experiments.

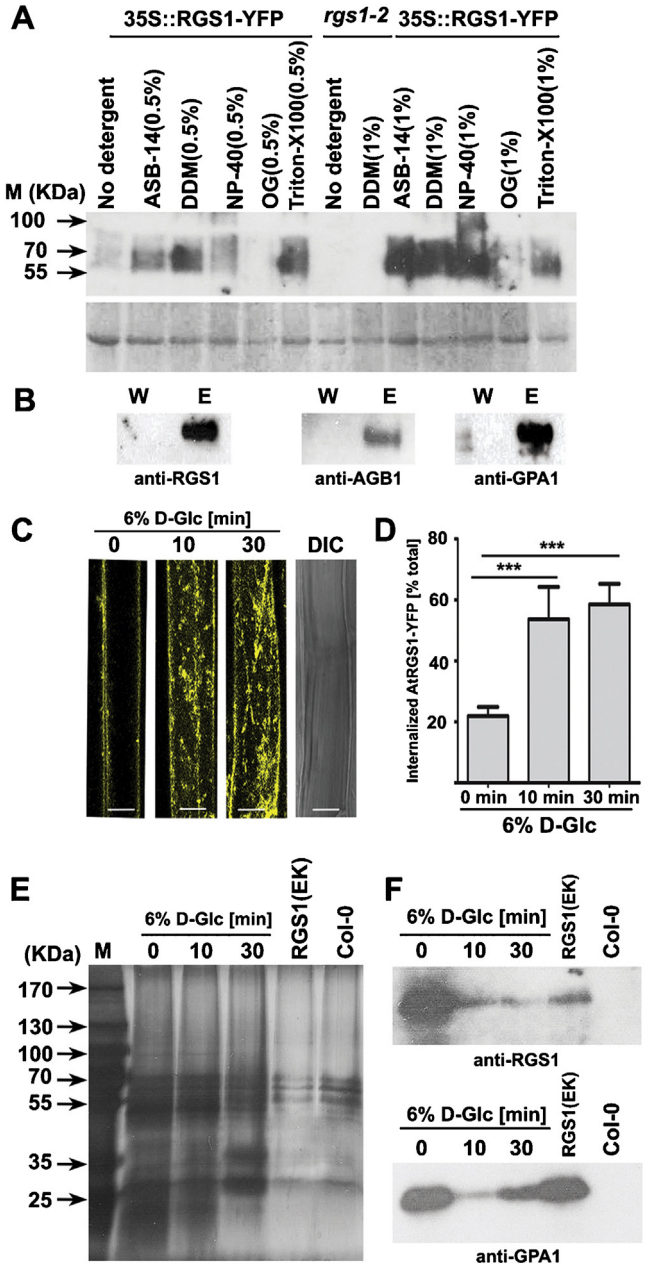

Fig. 2. Detergent screening and tandem affinity purification of AtRGS1-associated protein complex. (A) Western blots showing solubilization efficiency of AtRGS1–TAP using five different detergents at 0.5% and 1% concentrations. Approximately 20 μg of total membrane proteins were subjected to SDS PAGE and probed with anti-RGS1 antibody (upper panel). The lower panel represents the corresponding CBB stained membrane. (B) Pilot test for ABS-14 solubilization of core *Arabidopsis* G protein complex. The ABS-14-solubilized sample was interrogated with the indicated antisera to AtRGS1, AtGPA1, and AGB1. (C, D) *Arabidopsis* seedlings stably expressing AtRGS1-YFP were treated with 6% D-glucose in presence of cycloheximide (70 μM) and internalization was imaged by confocal microscopy (C) and quantified (D). (E) Total membrane samples were prepared from untreated (Col 0 and 35S:AtRGS1E320K-TAP) and treated seedlings (35S:AtRGS1-TAP, 6% D-Glucose, 0, 10 and 30 min). Protein complexes were purified using the TAP protocol described in Section 2. Eluted fractions were precipitated by chloroform/methanol, separated by gel electrophoresis, and proteins were detected by silver staining as described in Section 2 (E). Co-purification of AtRGS1 and associated complexes were monitored by immunoblot analysis using anti-RGS1 and anti-GPA1 antibodies. W, washthrough before final elution; E, final eluate.

Please cite this article in press as: D.K. Jaiswal, et al., Time-dependent, glucose-regulated *Arabidopsis* Regulator of G-protein Signaling 1 network, Curr. Plant Biol. (2015), http://dx.doi.org/10.1016/j.cpb.2015.11.002

Sustained activation of G-protein signaling in *Arabidopsis* has been quantified by endocytosis of AtRGS1 in response to sugar and salt in single seedling experiments [7,18]. For this proteomic study, it was necessary to scale up to thousands of seedlings per sample. Therefore to determine if the biological response survives scale up, we examined AtRGS1-YFP internalization in the treatment format required here. Transgenic *Arabidopsis* expressing AtRGS1-YFP were treated in bulk with 6% D-glucose and internalization was analyzed at 10 min and 30 min by confocal microscopy. Approximately 60% of AtRGS1 was internalized within 30 min of treatment (Fig. 2C and D), consistent with previous studies [7]. Therefore, we conclude that the scaled-up format used for the proteomics analysis is sufficient to recapitulate AtRGS1 endocytosis that has been extensively quantified at the single seedling level.

3.2. Pilot-scale proteome for validated partners used to set large scale filtering criteria

Establishing excellent experimental and downstream processing conditions is a prerequisite for development of affinity capture based proteome studies, especially when dealing with seven transmembrane proteins. In animal systems, different strategies have been used to identify membrane-associated complexes such as use of biotinylated ligands to purify protein complexes [44], interaction motifs [45] and tandemly-tagged full length receptor protein [29]. However, these kinds of analyses with multi transmembrane proteins are rare in plants [46]. In fact, membrane proteome data sets describing various threshold parameters associated with high confidence interactomes *via* developer software such as SAINT are not available for plants. Therefore, to build a comprehensive and robust data set with optimal sensitivity to capture the maximum positive interactions of AtRGS1, we decided to identify and validate randomly selected candidates, which can be used later as an internal positive reference for SAINT analysis (see Section 3.4).

We used optimized conditions for large-scale purification of AtRGS1–TAP complexes and subsequent LC–MS/MS analyses for identification of validated-interacting partners. Proteins present in the complex were separated by one-dimensional-SDS-PAGE, and visualized using SYPRO Ruby staining (Fig. S1). During conventional IP experiments, immunoprecipitated proteins are usually separated on a 1D-SDS PAGE and only those proteins detected selectively in the experiment (*i.e.*, proteins observed in the experiment lane and not in the control lane) are subjected to further identification by mass spectrometry. However, this approach is error prone. We therefore used a more systematic approach in which each lane was systematically divided into different sections and manually excised. Corresponding gel sections excised from three biological replicates were pooled and then subjected to in-gel trypsin digestion and LC–MS/MS for identification. Several expected interacting proteins were identified in the AtRGS1–TAP purified sample including: WNK10, SALT-INDUCIBLE ZINC FINGER 1 (SZF1) and LOW EXPRESSION OF OSMOTICALLY RESPONSIVE GENES 1 (LOS1). The complete sets of proteins identified in this pilot experiment are listed in Table S1.

In order to obtain a set of validated AtRGS1 interactors needed to determine subsequent filtering criteria for large-scale proteome profiling, 7 candidates were randomly selected for testing using mating-based split-ubiquitin yeast two hybrid system. The full length AtRGS1 was fused to the Cub domain, while the full length candidate prey proteins were fused to the NubG domain. The interaction was determined by cell growth on selective medium lacking leucine, tryptophan, histidine, and adenine. We used varying concentrations of methionine in selective medium to increase selection stringency. Of the seven tested, four were confirmed to interact with AtRGS1 as indicated by growth on selective medium (Fig. 3). These were ADP-ribosylation factor A1E (ARFA1E, At3G62290), aquaporin PIP2-1 (At3g53420), 14-3-3-like protein GF14 phi (At1g35160), and ras-related protein RABB1c (At4g17170). Aquaporins are well known channel proteins with diverse subcellular localizations. They are involved in hydraulic regulation in response to various stimuli [47]. General regulatory factors (GRFs *i.e.*, 14-3-3) are highly conserved proteins, bind to phosphorylated proteins to modulate their function and have been implicated in diverse physiological functions in plants [48]. ARFA1E and RABB1c are members of a small GTPases superfamily and play an important role as regulators in membrane trafficking [49]. The validation rate is 57% (4/7 in Y2H, Fig. 3), which is conservatively low, it is to be noted that Y2H assay is sensitive to orientation of the split ubiquitin tags and does not detect post-translational modification-dependent interactions. These four candidates were used as internal positive standards for the subsequent full-scale experiment.

3.3. Identification of AtRGS1-associated proteins by mass spectrometry

Each of three time points sampled included 3 biological replicates with 3 technical replicates each. Biological samples were taken at 0, 10, and 30 min after glucose addition to the seedlings as described in Section 2. We also included a TAP-tagged AtRGS1 mutant having a single glutamic (E320) mutated to lysine. This glutamic acid residue is critical for AtRGS1 interaction with the Gα subunit. This mutation abolishes the GAP activity of the AtRGS protein [3], however it does not disrupt its interaction with Gα subunit at the plasma membrane [9]. AtRGS1 (E320K) mutated proteins do not leave the plasma membrane upon acute D-glucose treatment [7]. Two negative controls were included: (1) untransformed Col-0 seedlings and (2) Col-0 expressing ACCELERATED CELL DEATH 2 (ACD2) tagged with TAP (ACD2-TAP) [28]. ACD2-TAP is a good negative control because it is associated with the chloroplast membrane fraction [28] and has the same TAP backbone as in AtRGS1–TAP. To acquire sufficient material for triplicate sampling *via* LC–MS/MS analysis, protein complexes were purified from nine independent IP experiments for each biological condition [RGS1-TAP (0, 10, 30 min 6% Glc), RGS1 (E320K)-TAP, ACD2-TAP and wild type] and grouped into three separate replicates per biological condition for downstream handling. The complete list of identified proteins is presented in Table S2.

3.4. Construction of the glucose-induced AtRGS1 interactome

In order to construct a high quality interactome from the proteomics data, we performed 'significance analysis of interactome' (SAINT) analysis [50], a probabilistic scoring method to filter out non-specific interactions. Since little is known about validated AtRGS1 protein interactions, we optimized the selection of SAINT thresholds using the four validated proteins (Fig. 3) from the pilot run. The AvgP of validated candidate proteins were assessed and based on these values of internal candidates, we set a lower SAINT cut off score for all the datasets accordingly. Previous literature reports with the use of SAINT cut off score (AvgP $\geq$ 0.5) for interactome analysis [51–53]; however, we assessed the distribution of SAINT probability scores and accepted only those proteins showing a significantly-enriched SAINT score of 0.3 or higher (Table S3). The applied threshold is more lenient, however this might be necessary because of the penalty SAINT puts on interactions not detected in all replicates severely reduces the avgP score. This may also increase the false positive interactions. The control data sets were included from ACD2-TAP and Col-0 plants not expressing TAP-tagged AtRGS1. The SAINT scores and spectrum counts for all proteins assigned to each affinity purification and controls are provided in Table S3. The analysis revealed 119 proteins significantly

Please cite this article in press as: D.K. Jaiswal, et al., Time-dependent, glucose-regulated *Arabidopsis* Regulator of G-protein Signaling 1 network, Curr. Plant Biol. (2015), http://dx.doi.org/10.1016/j.cpb.2015.11.002

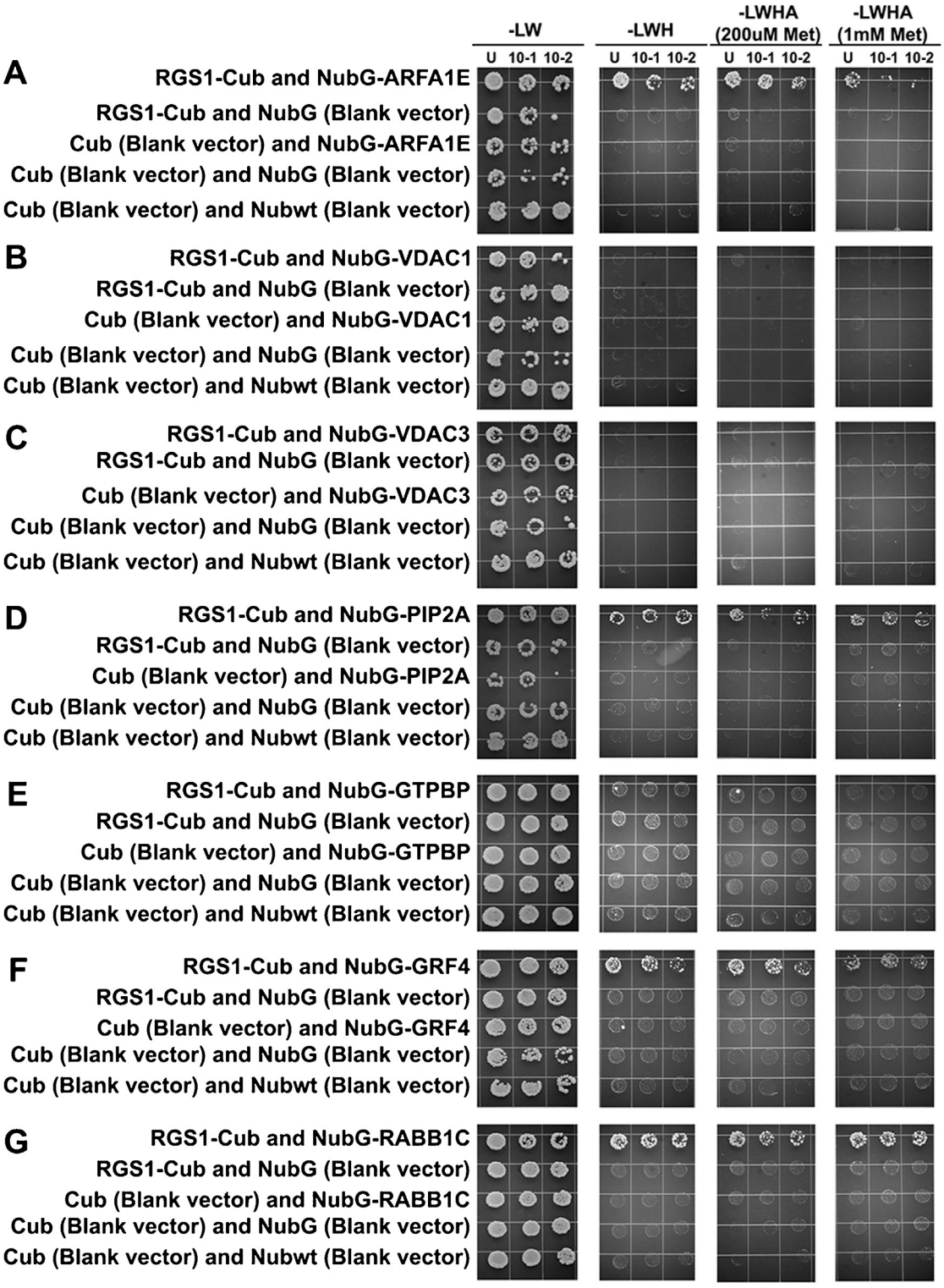

Fig. 3. Validation of candidate interactors from the pilot run. *In vivo* interaction for a random test set of complex components were tested using yeast complementation as described in Section 2. AtRGS1 physically interacts with AtARFA1 E (A), AtPIP2A (D), AtGRF4 (F), and AtRABB1 c (G) in yeast, detected using mating-based split ubiquitin system. Yeast THY.AP4 and THY.AP5 clones expressing full-length AtRGS1 and different complex proteins, respectively were mated. Yeast growth was observed in different selection media. L, leucine; W, tryptophan; H, histidine; A, adenine; Met, methionine; U, undiluted cells; 10^{-1} and 10^{-2} are sequential dilution of cells.

enriched during affinity purification; however we also observed a number of common and unique proteins (Fig. 4). Most of the proteins were identified from the untreated AtRGS1–TAP enrichment (6% Glc, 0 min) of which 74 proteins (64%) was uniquely assigned to this bait for this condition. Other conditions such as 10 and 30 min had the smallest number of proteins assigned to their enrichments [6 proteins (5%) and 19 proteins (16%)], respectively (Table S3). The interaction of AtRGS1 with Y2H validated protein/isoforms were observed in due course of D-glucose treatment. For example, the family members of aquaporin and general regulatory factors (GRF)

Please cite this article in press as: D.K. Jaiswal, et al., Time-dependent, glucose-regulated *Arabidopsis* Regulator of G-protein Signaling 1 network, Curr. Plant Biol. (2015), http://dx.doi.org/10.1016/j.cpb.2015.11.002

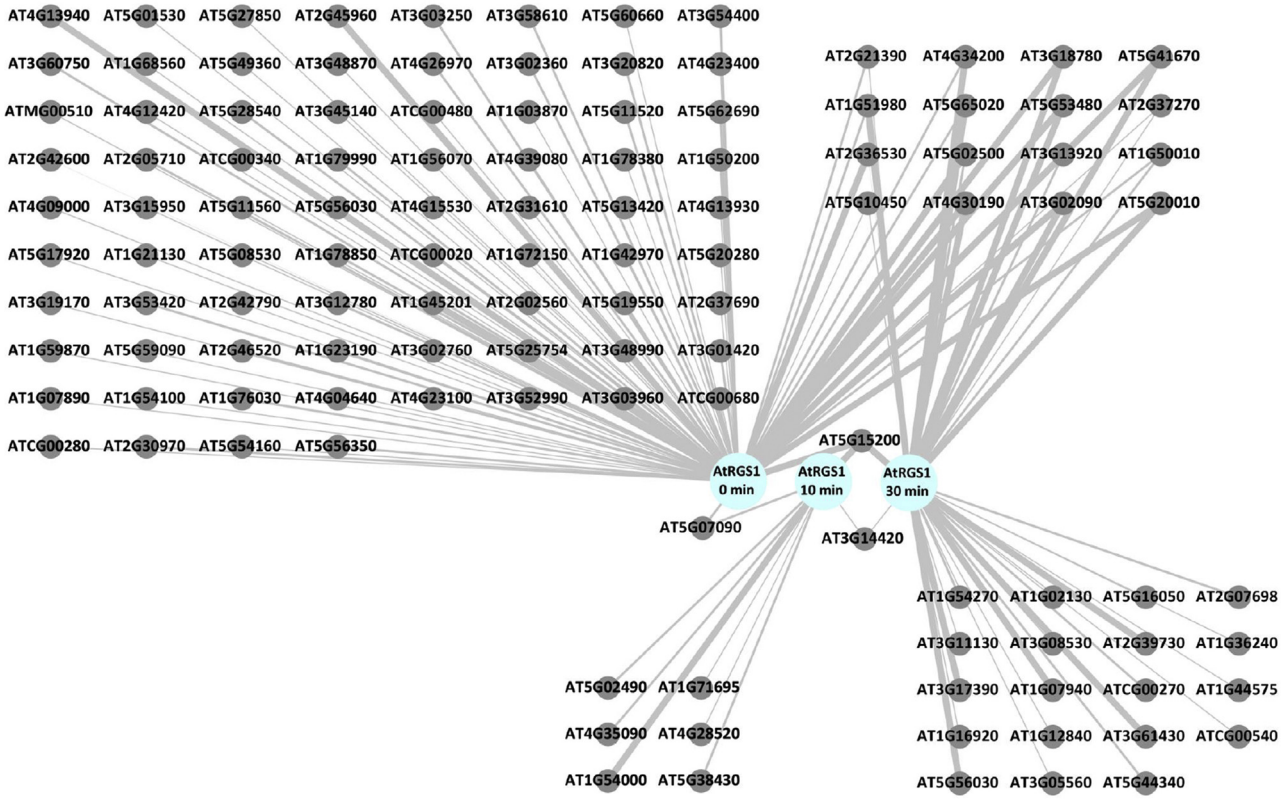

Fig. 4. Network analysis of AtRGS1 complex proteins. A total of 119 proteins obtained from three independent IP-MS experiments showing the dynamics of the AtRGS1-associated complex following treatment with glucose. Nodes represent proteins detected in IP-MS experiments whereas edges (lines connecting different nodes) indicate protein–protein interaction. Edge thickness is proportional to the average probability of interaction (avgP) determined by SAINT analysis.

interact with AtRGS1 at 0 min and 30 min time points; however the family member of small GTPase, RAB protein isoform, was found to be associated with AtRGS1 at 30 min following D-glucose treatment (Table S3). We developed a separate interactome map for the AtRGS1 (E320K) mutant (Fig. S3). SAINT analysis was performed as mentioned above using ACD2-TAP and Col-0 as the negative controls. The SAINT filtered prey data sets (Table S3) were analyzed using the *Arabidopsis* G-protein interactome database which showed that 21% of the proteins/isoforms identified as candidates of AtRGS1 complex were previously reported to be involved in the interaction with G-protein signaling components by yeast complementation assays [Y2H and Y3H, 24].

3.5. *Functional annotation of AtRGS1-associated proteins*

For functional categorization of candidate proteins, we applied GO analysis using the PlantGSEA search algorithm. TAIR accession numbers of the SAINT filtered list were submitted to PlantGSEA and GO terms with associated *p*-values were obtained (Table S4). Statistically overrepresented GO terms were subjected to REVIGO analyses for visualization of various processes [39]. The input list of proteins based on *p*-values was broadly grouped into biological processes (Fig. 5A), cellular component (Fig. 5B) and molecular function (Fig. 5C). In biological process, the most enriched GO terms associated with AtRGS1 complex protein were "response to metal ion", "generation of precursor metabolites and energy", "glucose metabolic pathway" and "response to stimulus" (Fig. 5A). In terms of cellular components, these proteins were distributed in different cellular and subcellular components. A broad-spectrum distribution of proteins were observed as evident from "membrane", "cytoplasm", "plasmodesma", "plastid", and "plasma membrane" (Fig. 5B). Molecular function classification revealed an overrepresentation of GO terms associated with "catalytic activity" and "nucleotide binding" as shown in Fig. 5C.

4. Discussion

Analysis of G protein interactome [25] showed that 149 candidates can directly interact with AtRGS1, whereas membrane-based interactome database showed 126 interactors in Y2H screen [54]. In this study, 119 proteins were identified as candidates of AtRGS1 complex protein *in vivo*. The validation rate of AtRGS1 complex protein interaction based on Y2H confirmation of our pilot screen was ~60% (Fig. 3). Twenty one percent of proteins identified from large screen (Table S3) were reported in the previous Y2H screen for AtRGS1/G-protein interacting proteins [25,54]. This clearly shows that many of them identified here (~80%, Table S3) are possibly novel candidates for AtRGS1complex proteins [25,54]. For example, the yeast two-hybrid screen using AtRGS1 as bait did not identify 14-3-3 proteins as identified and validated as an AtRGS1 interactor here (Fig. 3). Furthermore, some proteins that associate with AtRGS1 indirectly through other AtRGS1-binding proteins or in a post-translational modification dependent manner were identified by affinity purification but were not identified by yeast two-hybrid assays. For example, while no evidence exists for a direct interaction between LOS1 with AtRGS1, LOS1 interacts with the AtRGS1 partner, AtGPA1 [25]. This suggests that novel AtRGS1-associated proteins identified in this study might interact indirectly through other AtRGS1-interacting proteins, and thus have a function in AtRGS1-regulated processes. Furthermore, the copurification of enolase 2 known to interact with AGB1 [25], suggests that the AtRGS1-signaling components exist in a multi-protein complex and possibly involve adapter proteins hitherto undiscovered. V-ATPase c subunit (VHA-c) detected here is an interesting target because

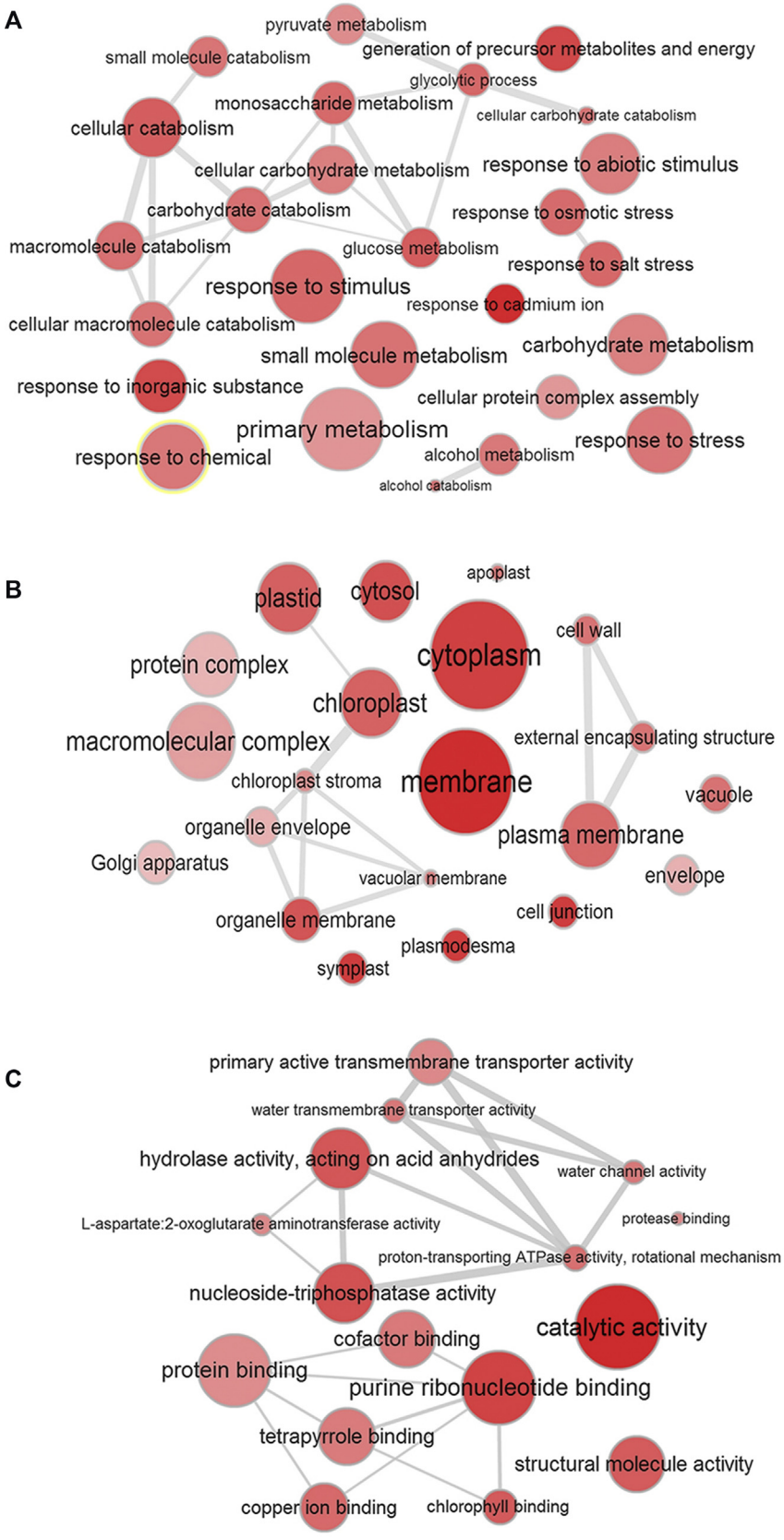

Fig. 5. Functional annotation of AtRGS1 complex proteins. GO term of SAINT analyzed AtRGS1 complex proteins were obtained using the Plant GeneSet Enrichment Analysis Toolkit. Interactive graph of over-represented GO terms were visualized by REVIGO. (A) biological process, (B) cellular component, and (C) molecular function.

Please cite this article in press as: D.K. Jaiswal, et al., Time-dependent, glucose-regulated *Arabidopsis* Regulator of G-protein Signaling 1 network, Curr. Plant Biol. (2015), http://dx.doi.org/10.1016/j.cpb.2015.11.002

functionally active VHA-c is required for proper localization of AtRGS1 on the plasma membrane [55].

Ligand-dependent endocytosis of GPCRs in animal cells may or may not require clathrin [56,57]. Clathrins are highly conserved coat proteins involved in the endocytic pathway regulating protein abundance at the plasma membrane and or the trans-Golgi network during cellular signaling [58]. While it is well known that sugar induces endocytosis of AtRGS1, it was not known whether AtRGS1 endocytosis is clathrin dependent or independent. We observed the association of AtRGS1 with the vesicle coat protein clathrin heavy chain 1 (At3g11130) and 2 (At3g08530) 30 min after D-glucose treatment (Table S3) indicating RGS1 endocytosis is clathrin dependent. Consistent with an endocytic role for AtRGS1, clathrin proteins were associated with AtRGS1 following D-glucose treatment.

In animals, agonists induce GPCR internalization in a phosphorylation-dependent manner. Phosphorylated GPCRs are recognized by a group of proteins called arrestin and arrestin-fold containing proteins designated VPS proteins [59,60]; both types recruit adaptor protein complex which then recruit clathrin triskelions to initiate endocytosis [61]. Endocytosis of animal GPCRs sequesters the GPCR away from the external stimulus, leading to signal desensitization. However, signaling also occurs at the endosome [62,63]. The possible fates of endocytosed proteins are (1) recycled back to the plasma membrane, (2) transported to the lysosome for degradation, and (3) retrograde transported to the trans-Golgi network [64]. RAB (Ras-like small GTP binding) and ARF (ADP-ribosylation factor) are small GTP-binding proteins and well characterized in vesicular trafficking [49]. During endocytosis, Ras-like GTPase family members selectively associate with recycling and sorting endosomes [49,65], whereas ARF family members bind to the target and recruit adapter protein AP-2 and consequently clathrin [66]. ARF proteins are not only involved in the endocytosis of GPCRs [67,68] but also in recycling from endosomes [69]. Since AtRGS1 interacts with members of the RAB and ARF families of small GTPases (Fig. 3), we hypothesize that interaction with these molecules play an important role in the initiation of endocytosis of AtRGS1 as well as its recycling back to the plasma membrane. We further propose that AtRGS1 promotes continued signaling from endosomes as evidenced from the interaction of RAB member with the receptor on endosomes appearing to be important for inhibition of the internalized receptor to lysosomes [70].

In animal cells, 14-3-3 proteins bind to the phosphorylated RGS protein to inhibit the GAP activity [71]. We show here that AtRGS1 interacts with a 14-3-3 protein. This 14-3-3 protein likely provides additional regulation of G-protein signaling either at the plasma membrane and/or from endosomes. Family members of this protein were identified during untreated as well as following D-glucose treatment. By analogy, once AtRGS1 is phosphorylated, 14-3-3 protein may bind to the phosphorylated form of AtRGS1 to inhibit its GAP activity, allowing the "self-activation" of AtGPA1 and consequently G-protein signaling.

Many candidate proteins were identified with other cellular functions. These proteins include water channels (*e.g.*, aquaporin), transporters [*e.g.*, H+-ATPase (AHA) and ABC transporter ABCG.36], chaperones (*e.g.*, HSP90-2 and HSP70-1), and metabolic enzymes (*e.g.*, enolase, pyruvate kinase and phosphoglycerate kinase) among others. Although the presence of metabolic enzymes and proteins from the chloroplast in the AtRGS1 interactome is surprising, many of them were found to interact with AtRGS1/G-protein signaling complex in Y2H [25]. The biological implications of the interactions between AtRGS1 and these proteins are yet to be determined.

The charge reversal mutant of AtRGS1 (E320K) disrupts the GTPase accelerating activity and glucose-induced endocytosis but not the interaction with AtGPA1 [3]. Some of the partners to AtRGS1 are shared by the AtRGS1(E320K) mutant such as aquaporin. As expected, proteins associated with endocytosis and membrane trafficking were not detected in the AtRGS1 (E320K) network. AtGPA1 was associated with the AtRGS1 (E320K) complex (Fig. 2F) indicating the presence of multiple interaction interfaces. Given the presence of the 7-transmembrane domain, it is plausible that AtRGS1 structure is unique and provides a novel interaction interface with AtGPA1 and other interactor molecules as the original yeast complementation results suggested [5].

The dynamic properties of the D-glucose-regulated AtRGS1 signaling networks are likely modulated by AtRGS1 internalization, which depend on the dose and duration of sugar applied [8]. A high dose of glucose was applied to shorten the window of time for glucose-induced endocytosis of AtRGS1. Our result shows that the AtRGS1 interactome changes in minutes of glucose application. AtRGS1 is initially associated with a group of protein involved in transport, stress and metabolism. Immediately after glucose addition, there is a recruitment of proteins that stimulate the endocytic pathways (Table S3) and therefore promote downstream signaling events. By 30 min, the AtRGS1 complex is dramatically altered and increased in size. These later complex components include annexin, 14-3-3, aquaporin, clathrin and ras-like GTPases among others (Table S3). We speculate that this change in the composition of the AtRGS1 complex leads to signaling originating from the endosome.

Conflicts of interest

The authors have declared no conflicts of interest.

Acknowledgements

Work in the Jones Lab is supported by grants from the NIGMS (R01GM065989), and NSF (MCB-0723515, MCB-1158054, and MCB-0718202). The Division of Chemical Sciences, Geosciences, and Biosciences, Office of Basic Energy Sciences of the US Department of Energy provided technical support for this study (DE-FG02-05er15671). We thank Dr. Daisuke Urano for his helpful comments, Dr. Meral Tunc-Ozdemir for confocal analysis of AtRGS1 internalization and Ms. Jing Yang for her technical assistance.

Appendix A. Supplementary data

Supplementary data associated with this article can be found, in the online version, at http://dx.doi.org/10.1016/j.cpb.2015.11.002.

References

[1] D. Urano, J.G. Chen, J.R. Botella, A.M. Jones, Heterotrimeric G protein signalling in the plant kingdom, Open Biol. 3 (2013) 120186.
[2] T.M. Cabrera-Vera, J. Vanhauwe, T.O. Thomas, M. Medkova, A. Preininger, M.R. Mazzoni, H.E. Hamm, Insights into G protein structure function, and regulation, Endocr. Rev. 24 (2003) 765–781.
[3] C.A. Johnston, J.P. Taylor, Y. Gao, A.J. Kimple, J.C. Grigston, J.G. Chen, D.P. Siderovski, A.M. Jones, F.S. Willard, GTPase acceleration as the rate-limiting step in *Arabidopsis* G protein-coupled sugar signaling, Proc. Natl. Acad. Sci. U. S. A. 104 (2007) 17317–17322.
[4] W. Bradford, A. Buckholz, J. Morton, C. Price, A.M. Jones, D. Urano, Eukaryotic G protein signaling evolved to require G protein-coupled receptors for activation, Sci. Signal. 6 (2013) ra37.
[5] J.G. Chen, F.S. Willard, J. Huang, J. Liang, S.A. Chasse, A.M. Jones, D.P. Siderovski, A seven-transmembrane RGS protein that modulates plant cell proliferation, Science 301 (2003) 1728–1731.
[6] D. Urano, A.M. Jones, Heterotrimeric G protein-coupled signaling in plants, Annu. Rev. Plant Biol. 65 (2014) 365–384.
[7] D. Urano, N. Phan, J.C. Jones, J. Yang, J. Huang, J. Grigston, J.P. Taylor, A.M. Jones, Endocytosis of the seven-transmembrane RGS1 protein activates G-protein-coupled signalling in *Arabidopsis*, Nat. Cell Biol. 14 (2012) 1079–1088.

Please cite this article in press as: D.K. Jaiswal, et al., Time-dependent, glucose-regulated *Arabidopsis* Regulator of G-protein Signaling 1 network, Curr. Plant Biol. (2015), http://dx.doi.org/10.1016/j.cpb.2015.11.002

[8] Y. Fu, S. Lim, D. Urano, M. Tunc-Ozdemir, N.G. Phan, T.C. Elston, A.M. Jones, Reciprocal encoding of signal intensity and duration in a glucose-sensing circuit, Cell 156 (2014) 1084–1095.
[9] J.C. Grigston, D. Osuna, W.R. Scheible, C. Liu, M. Stitt, A.M. Jones, D-Glucose sensing by a plasma membrane regulator of G signaling protein, AtRGS1, FEBS Lett. 582 (2008) 3577–3584.
[10] R. Irannejad, J.C. Tomshine, J.R. Tomshine, M. Chevalier, J.P. Mahoney, J. Steyaert, S.G. Rasmussen, R.K. Sunahara, H. El-Samad, B. Huang, M. von Zastrow, Conformational biosensors reveal GPCR signalling from endosomes, Nature 495 (2013) 534–538.
[11] J.G. Chen, Y. Gao, A.M. Jones, Differential roles of *Arabidopsis* heterotrimeric G-protein subunits in modulating cell division in roots, Plant Physiol. 141 (2006) 887–897.
[12] D. Urano, A. Colaneri, A.M. Jones, Galpha modulates salt-induced cellular senescence and cell division in rice and maize, J. Exp. Bot. 65 (2014) 6553–6561.
[13] H. Ullah, J.G. Chen, B. Temple, D.C. Boyes, J.M. Alonso, K.R. Davis, J.R. Ecker, A.M. Jones, The beta-subunit of the *Arabidopsis* G protein negatively regulates auxin-induced cell division and affects multiple developmental processes, Plant Cell 15 (2003) 393–409.
[14] Y. Fujisawa, T. Kato, S. Ohki, A. Ishikawa, H. Kitano, T. Sasaki, T. Asahi, Y. Iwasaki, Suppression of the heterotrimeric G protein causes abnormal morphology including dwarfism, in rice, Proc. Natl. Acad. Sci. U. S. A. 96 (1999) 7575–7580.
[15] J.F. Botto, S. Ibarra, A.M. Jones, The heterotrimeric G-protein complex modulates light sensitivity in *Arabidopsis thaliana* seed germination, Photochem. Photobiol. 85 (2009) 949–954.
[16] H. Zhang, Z. Gao, X. Zheng, Z. Zhang, The role of G-proteins in plant immunity, Plant Signal. Behav. 7 (2012) 1284–1288.
[17] M.N. Aranda-Sicilia, Y. Trusov, N. Maruta, D. Chakravorty, Y. Zhang, J.R. Botella, Heterotrimeric G proteins interact with defense-related receptor-like kinases in *Arabidopsis*, J. Plant Physiol. 188 (2015) 44–48.
[18] A.C. Colaneri, M. Tunc-Ozdemir, J.P. Huang, A.M. Jones, Growth attenuation under saline stress is mediated by the heterotrimeric G protein complex, BMC Plant Biol. 14 (2014), http://dx.doi.org/10.1186/1471-2229-14-129.
[19] Y. Yu, S.M. Assmann, The heterotrimeric G-protein beta subunit AGB1, plays multiple roles in the *Arabidopsis* salinity response, Plant Cell Environ. 38 (2015) 2143–2156.
[20] A. Wingler, S. Purdy, J.A. MacLean, N. Pourtau, The role of sugars in integrating environmental signals during the regulation of leaf senescence, J. Exp. Bot. 57 (2006) 391–399.
[21] W.H. Cheng, E.W. Taliercio, P.S. Chourey, Sugars modulate an unusual mode of control of the cell-wall invertase gene (Incw1) through its 3′ untranslated region in a cell suspension culture of maize, Proc. Natl. Acad. Sci. U. S. A. 96 (1999) 10512–10517.
[22] M.R. Bolouri Moghaddam, W. Van den Ende, Sugars and plant innate immunity, J. Exp. Bot. 63 (2012) 3989–3998.
[23] I. Morkunas, L. Ratajczak, The role of sugar signaling in plant defense responses against fungal pathogens, Acta Physiol. Plant. 36 (2014) 1607–1619.
[24] J.C. Jones, J.W. Duffy, M. Machius, B.R. Temple, H.G. Dohlman, A.M. Jones, The crystal structure of a self-activating G protein alpha subunit reveals its distinct mechanism of signal initiation, Sci. Signal. 4 (2011) ra8.
[25] K. Klopffleisch, N. Phan, K. Augustin, R.S. Bayne, K.S. Booker, J.R. Botella, N.C. Carpita, T. Carr, J.G. Chen, T.R. Cooke, A. Frick-Cheng, E.J. Friedman, B. Fulk, M.G. Hahn, K. Jiang, L. Jorda, L. Kruppe, C. Liu, J. Lorek, M.C. McCann, A. Molina, E.N. Moriyama, M.S. Mukhtar, Y. Mudgil, S. Pattathil, J. Schwarz, S. Seta, M. Tan, U. Temp, Y. Trusov, D. Urano, B. Welter, J. Yang, R. Panstruga, J.F. Uhrig, A.M. Jones, *Arabidopsis* G-protein interactome reveals connections to cell wall carbohydrates and morphogenesis, Mol. Syst. Biol. 7 (2011) 532.
[26] A. Bruckner, C. Polge, N. Lentze, D. Auerbach, U. Schlattner, Yeast two-hybrid, a powerful tool for systems biology, Int. J. Mol. Sci. 10 (2009) 2763–2788.
[27] S.J. Clough, A.F. Bent, Floral dip: a simplified method for *Agrobacterium*-mediated transformation of *Arabidopsis thaliana*, Plant J. 16 (1998) 735–743.
[28] Y. Sakuraba, S. Schelbert, S.Y. Park, S.H. Han, B.D. Lee, C.B. Andres, F. Kessler, S. Hortensteiner, N.C. Paek, STAY-GREEN and chlorophyll catabolic enzymes interact at light-harvesting complex II for chlorophyll detoxification during leaf senescence in *Arabidopsis*, Plant Cell 24 (2012) 507–518.
[29] A.M. Daulat, P. Maurice, C. Froment, J.L. Guillaume, C. Broussard, B. Monsarrat, P. Delagrange, R. Jockers, Purification and identification of G protein-coupled receptor protein complexes under native conditions, Mol. Cell. Proteom. 6 (2007) 835–844.
[30] J.P. Seifert, Y. Zhou, S.N. Hicks, J. Sondek, T.K. Harden, Dual activation of phospholipase C-epsilon by Rho and Ras GTPases, J. Biol. Chem. 283 (2008) 29690–29698.
[31] D. Friedman, K. Lilley, Optimizing the Difference Gel Electrophoresis (DIGE) Technology, in: A. Vlahou (Ed.), Humana Press, 2008, pp. 93–124.
[32] S. Alvarez, B.M. Berla, J. Sheffield, R.E. Cahoon, J.M. Jez, L.M. Hicks, Comprehensive analysis of the *Brassica juncea* root proteome in response to cadmium exposure by complementary proteomic approaches, Proteomics 9 (2009) 2419–2431.
[33] W.O. Slade, E.G. Werth, E.W. McConnell, S. Alvarez, L.M. Hicks, Quantifying reversible oxidation of protein thiols in photosynthetic organisms, J. Am. Soc. Mass Spectrom. 26 (2015) 631–640.
[34] G. Liu, J. Zhang, B. Larsen, C. Stark, A. Breitkreutz, Z.Y. Lin, B.J. Breitkreutz, Y. Ding, K. Colwill, A. Pasculescu, T. Pawson, J.L. Wrana, A.I. Nesvizhskii, B. Raught, M. Tyers, A.C. Gingras, ProHits: integrated software for mass spectrometry-based interaction proteomics, Nat. Biotechnol. 28 (2010) 1015–1017.
[35] G. Teo, G. Liu, J. Zhang, A.I. Nesvizhskii, A.C. Gingras, H. Choi, SAINTexpress: improvements and additional features in significance analysis of INTeractome software, J. Proteom. 100 (2014) 37–43.
[36] H. Choi, G. Liu, D. Mellacheruvu, M. Tyers, A.C. Gingras, A.I. Nesvizhskii, Analyzing protein-protein interactions from affinity purification-mass spectrometry data with SAINT, Curr. Protoc. Bioinform. (2012), Chapter 8, Unit8.15.
[37] C.T. Lopes, M. Franz, F. Kazi, S.L. Donaldson, Q. Morris, G.D. Bader, Cytoscape, Web: an interactive web-based network browser, Bioinformatics 26 (2010) 2347–2348.
[38] X. Yi, Z. Du, Z. Su, PlantGSEA: a gene set enrichment analysis toolkit for plant community, Nucleic Acids Res. 41 (2013) W98–103.
[39] F. Supek, M. Bosnjak, N. Skunca, T. Smuc, REVIGO summarizes and visualizes long lists of gene ontology terms, PLoS One 6 (2011) e21800.
[40] S. Lalonde, A. Sero, R. Pratelli, G. Pilot, J. Chen, M.I. Sardi, S.A. Parsa, D.Y. Kim, B.R. Acharya, E.V. Stein, H.C. Hu, F. Villiers, K. Takeda, Y. Yang, Y.S. Han, R. Schwacke, W. Chiang, N. Kato, D. Loque, S.M. Assmann, J.M. Kwak, J.I. Schroeder, S.Y. Rhee, W.B. Frommer, A membrane protein/signaling protein interaction network for *Arabidopsis* version AMPv2, Front. Physiol. 1 (2010) 24.
[41] P. Obrdlik, M. El-Bakkoury, T. Hamacher, C. Cappellaro, C. Vilarino, C. Fleischer, H. Ellerbrok, R. Kamuzinzi, V. Ledent, D. Blaudez, D. Sanders, J.L. Revuelta, E. Boles, B. Andre, W.B. Frommer, K+ channel interactions detected by a genetic system optimized for systematic studies of membrane protein interactions, Proc. Natl. Acad. Sci. U. S. A. 101 (2004) 12242–12247.
[42] M. Babu, J. Vlasblom, S. Pu, X. Guo, C. Graham, B.D. Bean, H.E. Burston, F.J. Vizeacoumar, J. Snider, S. Phanse, V. Fong, Y.Y. Tam, M. Davey, O. Hnatshak, N. Bajaj, S. Chandran, T. Punna, C. Christopolous, V. Wong, A. Yu, G. Zhong, J. Li, I. Stagljar, E. Conibear, S.J. Wodak, A. Emili, J.F. Greenblatt, Interaction landscape of membrane-protein complexes in *Saccharomyces cerevisiae*, Nature 489 (2012) 585–589.
[43] S. Rivas, T. Mucyn, H.A. van den Burg, J. Vervoort, J.D. Jones, An approximately 400 kDa membrane-associated complex that contains one molecule of the resistance protein Cf-4, Plant J. 29 (2002) 783–796.
[44] P.J. Brown, A. Schonbrunn, Affinity purification of a somatostatin receptor–G-protein complex demonstrates specificity in receptor–G-protein coupling, J. Biol. Chem. 268 (1993) 6668–6676.
[45] C. Becamel, S. Gavarini, B. Chanrion, G. Alonso, N. Galeotti, A. Dumuis, J. Bockaert, P. Marin, The serotonin 5-HT2A and 5-HT2C receptors interact with specific sets of PDZ proteins, J. Biol. Chem. 279 (2004) 20257–20266.
[46] R.B. Rodrigues, G. Sabat, B.B. Minkoff, H.L. Burch, T.T. Nguyen, M.R. Sussman, Expression of a translationally fused TAP-tagged plasma membrane proton pump in *Arabidopsis thaliana*, Biochemistry 53 (2014) 566–578.
[47] C. Maurel, Y. Boursiac, D.T. Luu, V. Santoni, Z. Shahzad, L. Verdoucq, Aquaporins in plants, Physiol. Rev. 95 (2015) 1321–1358.
[48] F.C. Denison, A.L. Paul, A.K. Zupanska, R.J. Ferl, 14-3-3 Proteins in plant physiology, Semin. Cell Dev. Biol. 22 (2011) 720–727.
[49] E. Nielsen, A.Y. Cheung, T. Ueda, The regulatory RAB and ARF GTPases for vesicular trafficking, Plant Physiol. 147 (2008) 1516–1526.
[50] H. Choi, B. Larsen, Z.Y. Lin, A. Breitkreutz, D. Mellacheruvu, D. Fermin, Z.S. Qin, M. Tyers, A.C. Gingras, A.I. Nesvizhskii, SAINT: probabilistic scoring of affinity purification-mass spectrometry data, Nat. Methods 8 (2011) 70–73.
[51] S. Moon, D. Han, Y. Kim, J. Jin, W.K. Ho, Y. Kim, Interactome analysis of AMP-activated protein kinase (AMPK)-alpha1 and -beta1 in INS-1 pancreatic beta-cells by affinity purification-mass spectrometry, Sci. Rep. 4 (2014) 4376.
[52] M. Taipale, G. Tucker, J. Peng, I. Krykbaeva, Z.Y. Lin, B. Larsen, H. Choi, B. Berger, A.C. Gingras, S. Lindquist, A quantitative chaperone interaction network reveals the architecture of cellular protein homeostasis pathways, Cell 158 (2014) 434–448.
[53] D.V. Skarra, M. Goudreault, H. Choi, M. Mullin, A.I. Nesvizhskii, A.C. Gingras, R.E. Honkanen, Label-free quantitative proteomics and SAINT analysis enable interactome mapping for the human Ser/Thr protein phosphatase 5, Proteomics 11 (2011) 1508–1516.
[54] A.M. Jones, Y. Xuan, M. Xu, R.S. Wang, C.H. Ho, S. Lalonde, C.H. You, M.I. Sardi, S.A. Parsa, E. Smith-Valle, T. Su, K.A. Frazer, G. Pilot, R. Pratelli, G. Grossmann, B.R. Acharya, H.C. Hu, C. Engineer, F. Villiers, C. Ju, K. Takeda, Z. Su, Q. Dong, S.M. Assmann, J. Chen, J.M. Kwak, J.I. Schroeder, R. Albert, S.Y. Rhee, W.B. Frommer, Border control—a membrane-linked interactome of *Arabidopsis*, Science 344 (2014) 711–716.
[55] A. Zhou, Y. Bu, T. Takano, X. Zhang, S. Liu, Conserved V-ATPase c subunit plays a role in plant growth by influencing V-ATPase-dependent endosomal trafficking, Plant Biotechnol. J. (2015).
[56] M. Wan, W. Zhang, Y. Tian, C. Xu, T. Xu, J. Liu, R. Zhang, Unraveling a molecular determinant for clathrin-independent internalization of the M2 muscarinic acetylcholine receptor, Sci. Rep. 5 (2015) 11408.
[57] G. Lavezzari, K.W. Roche, Constitutive endocytosis of the metabotropic glutamate receptor mGluR7 is clathrin-independent, Neuropharmacology 52 (2007) 100–107.
[58] X. Chen, N.G. Irani, J. Friml, Clathrin-mediated endocytosis: the gateway into plant cells, Curr. Opin. Plant Biol. 14 (2011) 674–682.
[59] V.V. Gurevich, E.V. Gurevich, Structural determinants of arrestin functions, Prog. Mol. Biol. Transl. Sci. 118 (2013) 57–92.

Please cite this article in press as: D.K. Jaiswal, et al., Time-dependent, glucose-regulated *Arabidopsis* Regulator of G-protein Signaling 1 network, Curr. Plant Biol. (2015), http://dx.doi.org/10.1016/j.cpb.2015.11.002

[60] L. Aubry, D. Guetta, G. Klein, The arrestin fold: variations on a theme, Curr. Genom. 10 (2009) 133–142.
[61] F. Delom, D. Fessart, Role of phosphorylation in the control of clathrin-mediated internalization of GPCR, Int. J. Cell Biol. 2011 (2011) 246954.
[62] D. Calebiro, V.O. Nikolaev, L. Persani, M.J. Lohse, Signaling by internalized G-protein-coupled receptors, Trends Pharmacol. Sci. 31 (2010) 221–228.
[63] A. Sorkin, M. von Zastrow, Endocytosis and signalling: intertwining molecular networks, Nat. Rev. Mol. Cell Biol. 10 (2009) 609–622.
[64] V.W. Hsu, M. Bai, J. Li, Getting active: protein sorting in endocytic recycling, Nat. Rev. Mol. Cell Biol. 13 (2012) 323–328.
[65] J.L. Seachrist, S.S. Ferguson, Regulation of G protein-coupled receptor endocytosis and trafficking by Rab GTPases, Life Sci. 74 (2003) 225–235.
[66] M.T. Drake, S.K. Shenoy, R.J. Lefkowitz, Trafficking of G protein-coupled receptors, Circ. Res. 99 (2006) 570–582.
[67] E. Macia, M. Partisani, O. Paleotti, F. Luton, M. Franco, Arf6 negatively controls the rapid recycling of the beta2 adrenergic receptor, J. Cell. Sci. 125 (2012) 4026–4035.
[68] C. Reiner, N.M. Nathanson, The internalization of the M2 and M4 muscarinic acetylcholine receptors involves distinct subsets of small G-proteins, Life Sci. 82 (2008) 718–727.
[69] M. Prigent, T. Dubois, G. Raposo, V. Derrien, D. Tenza, C. Rosse, J. Camonis, P. Chavrier, ARF6 controls post-endocytic recycling through its downstream exocyst complex effector, J. Cell Biol. 163 (2003) 1111–1121.
[70] L.B. Dale, J.L. Seachrist, A.V. Babwah, S.S. Ferguson, Regulation of angiotensin II type 1A receptor intracellular retention degradation, and recycling by Rab5, Rab7, and Rab11 GTPases, J. Biol. Chem. 279 (2004) 13110–13118.
[71] M. Abramow-Newerly, H. Ming, P. Chidiac, Modulation of subfamily B/R4 RGS protein function by 14-3-3 proteins, Cell. Signal. 18 (2006) 2209–2222.

Please cite this article in press as: D.K. Jaiswal, et al., Time-dependent, glucose-regulated *Arabidopsis* Regulator of G-protein Signaling 1 network, Curr. Plant Biol. (2015), http://dx.doi.org/10.1016/j.cpb.2015.11.002